BEHAVIOR OF SURFACTANT MIXTURES AT SOLID/LIQUID AND OIL/LIQUID INTERFACES IN CHEMICAL FLOODING SYSTEMS

SEMIANNUALLY TECHNICAL   PROGRESS   REPORT

Reporting Period Start Date: 09/01/2002

Reporting Period End Date: 02/28/2003

Principle Author: Prof. P. Somasundaran

Date Report Issued: March 31, 2003

DOE Award Number: DE-FC26-01BC15312

**Principal
Investigator**   Prof. P. Somasundaran

Submitting Organization   Office of Projects and Grants
Columbia University in the City of New York
1210 Amsterdam Avenue, Mail Code 2205
Room 254 Engineering Terrace
New York, NY 10027

**Contracting Officer's
Representative**   H.V. Weyland
U.S. Department of Energy,
National Petroleum Technology Office
One West Third Street, Suit 1400
Tulsa, Oklahoma 74101-3519

DISCLAIMER

ABSTRACT

The aim of the project is to develop a knowledge base to help with the design of enhanced process for mobilizing and extracting untrapped oil. We emphasize on evaluating novel surfactant mixtures and on obtaining optimum combinations of the surfactants in chemical flooding EOR process. An understanding of the micellar shape and size is crucial since these physical properties directly determine the crude oil removal efficiency. Analytical ultracentrifugation experiments were used to test the multi-micelle model proposed earlier and formulate the relationships between mixed micelle formation and the surfactant structure. Information on partial specific volume of surfactants and their mixtures is required to treat analytical ultracentrifuge data. In the last report, it was noted that the partial specific volumes of the sugar-based surfactants obtained experimentally did not agree with those from theoretical calculations. A scrutiny of partial specific volumes of the four sugar-based surfactants revealed that conformational changes upon micelle formation are responsible for the large deviation. From sedimentation equilibrium experiments, two types of micelles were identified for the nonionic polyethylene surfactant and its mixtures with the sugar-based surfactant, dodecyl maltoside. The average aggregation numbers of n-dodecyl-β-D-maltoside and nonyl phenol ethoxylated decyl ether agreed with those reported in literature using other techniques. Our study displayed, for the first time, that small micelles might coexist with large micelles at high concentrations due to unique structures of the surfactant although classical thermodynamic theory supports only one type of micelle. Initial dynamic light scattering results support the results for the same mixed surfactant system from analytical ultracentrifuge equilibrium technique. The implication of this finding lies in the fact that efficiency of oil recovery will be improved due to the large micellar size, its polymer-like fluidity and possible reduced adsorption on solids.

TABLE OF CONTENTS

LIST OF GRAPHIC MATERIALS

INTRODUCTION

Considerable amount of oil is trapped on porous rocks together with water and gas in reservoirs after primary and secondary oil recovery processes. Among various chemical EOR methods, surfactant EOR is promising due to its high efficiency and possible low cost. The goal of this project is to develop and evaluate efficient <u>novel mixtures</u> of surfactants for improved oil recovery, especially in a complex <u>multi-component</u> systems containing oil, polymers, emulsifiers and inorganics in the system.

Currently maximum opportunity exists for establishing the structure-performance relationships and apply the knowledge to fine tune chemical reagent schemes. Our recent work has shown some surfactant mixtures to exhibit new aggregation behavior both in aqueous solutions and at the solid-liquid interfaces: co-existence of more than one type of mixed micelles in the same multi-surfactant solutions. This finding has both theoretical and practical implications in the sense of minimizing interfacial tension and increasing oil removal efficiency.

In our previous work, protocol for analytical centrifugation was established to characterize surfactants and their mixtures. Towards this purpose, analytical ultracentrifugation tests were first performed to identify the best analytical method, calculate the partial specific volume for molecular weight determination and collect information on single surfactant systems. Partial specific volumes were estimated by two experimental methods: density gradient ($d\rho/dc$) and partial molar volume (V_o). Results obtained using the two methods is within 0.5%. It was found that the partial specific volume is concentration dependent and sensitive to changes in temperature. Such information will in future be used to identify optimum surfactant systems. Three software, Optima™ XL-A/XL-I data analysis software, DCDT+ and Svedberg were compared for sedimentation velocity data analysis. The sedimentation coefficient and aggregation number of NP-10 were obtained from the above three

software and Svedberg were found to be the best. Surface tension measurements were performed to determine critical micellar concentrations (cmc) of n-dodecyl-β-D-maltoside (DM), nonyl phenol ethoxylated decyl ether (NP-10) and their 1:1 mixtures at 25°C. Results revealed no interaction between the two surfactants in the mixed micelles. Partial specific volume measurements also indicated no interaction in mixed micelles. Maximum adsorption density, area per molecule and free energy of micellization were also calculated and compared with values in the literature.

Our previous results showed that the partial specific volume of sugar-based surfactant obtained experimentally deviated from that obtained using theoretical calculations. Partial molar volume of four sugar-based surfactants were determined in an attempt to account for the discrepancy. From sedimentation equilibrium experiments, aggregation number of n-dodecyl-β-D-maltoside, nonyl phenol ethoxylated decyl ether and their 1:1 molar ratio mixture were obtained to test the co-existence of two types of micelles. Dynamic light scattering technique was also employed to supplement the results from analytical ultracentrifuge equilibrium technique. Such information on aggregation of surfactants is particularly important for identifying optimum oil displacement condition.

EXPERIMENTAL

Materials

Non-ionic sugar-based n-dodecyl-β-D-maltoside (DM) (>95% purity by thin layer chromatography) from Calbiochem (<0.05% dodecanol), n-dodecyl-β-D-maltotrioside (DTM) (>99.8% purity by HPLC) from Anatrace, and nonionic nonyl phenol ethoxylated decyl ether(NP-10) (>99% purity by HPLC) from Nikko Chemicals were used as received.

Refractive index matching liquid, decalin mixture of cis and trans (>98% purity), was purchased from Acros Organics. It was used to reduce light bending at the glass interfaces in dynamic light scattering experiments.

Water used in all the experiments was triple distilled, with a specific conductivity of less than $1.5\mu\Omega^{-1}$ and tested for the absence of organics using surface tension measurements.

Methods:

1. Theoretical & experimental methods for partial specific volume

Approach of Durchschlag and Zipper[2,3] is adopted to obtain the theoretical partial specific volume based on Traube's additivity principle and concept of volume increments for atoms. All the calculated partial specific volumes are at 25^0C.

Empirically, partial specific volume was obtained by determining the density difference over concentration. Densities of surfactant solutions were measured with an Anton Paar DMA 5000 densitometer. The principle involved measurement of the period of oscillation of a U-shape tube with the sample inside. The accuracies of the density and temperature data were $\pm5*10^{-6}$g/cm^3 and $\pm0.01^0$C, respectively. The instrument was calibrated at atmospheric pressure (1013 mbar) with air

4

and Anton Paar's standard water (=0.99820 ± 0.000010 g/cm³ at 20⁰C). Acetone was used to rinse

the U-tube between measurements and was dried by pumping filtered air into U-tube.

Partial specific volume played an important role in the determination of micellar mass by

analytical ultracentrifuge in that the quantity directly measured by sedimentation experiment was

the buoyant mass, $M(1 - \bar{v}\rho)$ If the solute concentration is determined on a mass/volume basis, the

digital densitometer can measure the partial specific volume to a deviation within 0.2%.

2. Theory and experimental scheme of analytical ultracentrifuge sedimentation equilibrium

The sedimentation equilibrium experiments require several criteria [8]:

a.   The sedimentation equilibrium is reached if the concentration distribution did not

change with time.

b.   The equilibrium distribution depended only on the buoyant molecular weight and not

in anyway on the shape of particles in solution.

c.   Sedimentation equilibrium experiment can provide information such as the state of

aggregation.

The equilibrium equation was derived from Lamm equation:

$$\frac{\partial C}{\partial t} = \frac{1}{r}\frac{\partial}{\partial r}\left[rD\frac{\partial C}{\partial r} - s\omega^2 r^2 C\right] = 0$$

Where, $\partial C/\partial r$ is the solute concentration gradient, r is the radius, D is the diffusion

coefficient, s is sedimentation coefficient, $\omega^2 r$ is centrifugal force field strength, c is the solute

concentration and M is the molecular weight

Since $1/r \neq 0$, the Lamm equation could be expressed as:

$$D\frac{\partial C}{\partial r} = s\omega^2 r\ Cdr$$

Separating variables and integrating the equation,

$$C_r = C_a \, exp[\frac{s\omega^2}{2D}(r^2 - a^2)]$$

where a is the radial reference distance, and C_a is the solute concentration or absorbance at

a.

From the Svedberg equation:

$$\frac{s}{D} = \frac{M(1 - \bar{v}\rho)}{RT}$$

where M is the molecular weight of macromolecule or aggregation mass of the surfactant

micelles, ρ is solvent density, v bar is the partial specific volume, R is the gas constant and T is the

absolute temperature.

Thus, $$C_r = C_a \, exp\{\frac{\omega^2}{2RT} M(1 - v\rho)\}(r^2 - a^2)$$

From the assumption that sedimentation and diffusion have reached a state of equilibrium,

the following equation can be derived for equilibrium:

$$\frac{M(1 - \bar{v}\rho)\omega^2}{2RT} = \frac{d \, lnC}{dr^2}$$

A plot of lnC versus r^2 should give a straight line with a slope related to M. A straight line

was achieved only with a single, ideal species. The line was not linear if multiple species,

aggregation or nonideal species were present. It is clear that the concentration of macrosolute with

radial distance is nonlinear with respect to the parameter of interest, the buoyant molecular weight

$M(1 - \bar{v}\rho)$.

Data analysis generally involves nonlinear least squares regression.

While in an ideal solution: the solute species are point particles, occupying no volume, and

interact only through collisions. Real solutions of macromolecules will exhibit thermodynamic

nonideality because of the excluded volume effect of macromolecules which usually occupy a

significant fraction of the volume. This case was especially severe for particles of high masses and extended shapes. Nonideality occurred often with charged macromolecules since the electrostatic force act over long distances.

Nonideality was concentration dependent, being larger at high concentrations. Quantitatively, the nonideality can be measured through the relationship between apparent M and concentration, using virial coefficients:

$$M_{app} = \frac{M}{1 + BMC + ...}$$

and

$$\frac{1}{M_{app}} = \frac{1}{M} + BC + ...$$

where M_{app} is the apparent molecular weight obtained from the data, B is the second virial coefficient and C is the weight concentration of the centrifuged sample. The minimum of B was in the range of $10^{-5} - 10^{-6}$.

Probably the best test for the homogeneity with respect to mass is based on the residuals following minimization of the sum of squared scatterings. If the data is fitted to a single ideal solute model, the residual is randomly distributed if the solution is ideal. Upward residuals indicate aggregation and downward residuals nonideality.

Sedimentation equilibrium experiments were performed in a Beckman Coulter Optima™ XL-I analytical ultracentrifuge equipped with both absorbance and interference optical detectors [4]. A six-sector cell and sapphire windows [5] were used for sedimentation equilibrium experiments. The aluminum cell was counter-balanced on An An-60 Ti rotor.

In the sedimentation equilibrium experiment, the sample solutions were subjected to centrifugation at speeds ranging from 3,000 to 40,000 rpm. "Subtract data" command in Optima® XL-I data analysis software "Origin 4.0" was used to detect the equilibrium state. The blank noise

was removed using software WinReed and then the new data set were sent back to Optima® XL-I

data analysis software "Origin 4.0" to do the analysis. All experiments were done at temperature of

25 ± 0.1^0C.

3. Theory and experiment of dynamic light scattering

Dynamic light scattering (DLS), known also as quasi elastic light scattering (QELS) and

photon correlation spectroscopy (PCS), was used to analyze fluctuations in the intensity of the

scattered light in the short time scale of microseconds to milliseconds caused by the diffusional or

Brownian motion of the scattering particles. The light scattering depends on a number of factors

including the difference between refractive index of the particles and the suspending liquid, the

particle size and shape, the viscosity of the suspending medium, the wavelength and power of the
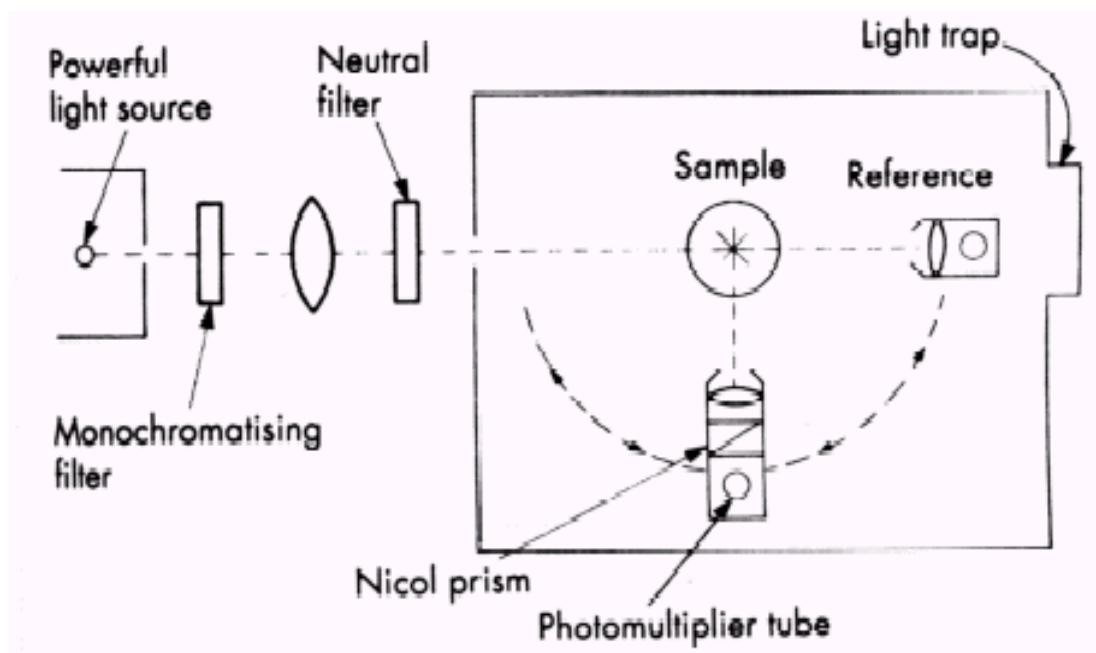
incident light, and the angle of measurement.

Figure 1. Schematics of light scattering apparatus (reproduced from [6])

DLS can typically provide the hydrodynamic diameter in the range of 2 nanometer up to 1000 nanometers, the translational diffusion coefficient, and the diffusional virial coefficient. The accuracy and precision of DLS vary based on the type of dispersion analyzed. For dust free samples, the precision is a few percent. Most experimental samples are not ideal, and involve polydispersity and dust contamination. Typical scatterings can be up to ±10%.

The presence of contaminant dust particles is probably the most significant factor affecting the accuracy and precision. The effects of dust can be addressed through extensive cleaning and filtration in the preparation of the samples and for some instruments, a software dust filter is used to eliminate scattered light intensities that suddenly increase in magnitude due to dust.

In the simplified case of two-particle systems, the incident monochromatic laser light is scattered by two particles that are separated by a distance, d [7]. The scattered light then travels to the photomultiplier tube and is converted to an electrical signal. The scattered wave fronts can have constructive or destructive interference according to the equation:

$$d \sin \theta = m\lambda$$

where d is distance between particles, θ is angle of scattering, m is constant, and λ is wavelength.

If m is an integer, then the optical interference is positive while if it is a half integer, the optical interference is destructive. The intensity of the scattered light I(t) varies from zero to two times the case for single particle scattering. A typical experimental sample has from 10^{7-8} particles so that there is random fluctuations between the two extremes. How fast the rate of variation in fluctuations vary determines the size of the particles.

The translational diffusion coefficient is determined from the scattering intensity time correlations function (TCF) $G2(t) = A + Bg_1^2(t)$

where A and B are constants and g_1^2 is the electric field TCF, given as

$$g_1 = \left| < E*(0)E(t) > \right| / \left| < E*(0)E(0) > \right|$$

E(0) and *E(t)* are the electric field amplitudes at zero time and delay time *t*. The asterisk denotes the conjugate complex quantity. The TCF shows an exponential-like decay to a base line *A*, and *B* is an efficiency parameter that is characteristic of the "signal to noise" ratio. Because of the exponential-like decay for $g_1(t)$, one can try to analyze the TCF via a cumulatant expansion given by [7]:

$$\ln g_1(t) = -\Gamma_1 t + (\Gamma_2 / 2!)t^2 - (\Gamma_3 / 3!)t^3 + ...$$

where $\Gamma = \Gamma_1$, Γ_2, Γ_3, ... are the first, second, third, etc. cumulants. The theory of dynamic light scattering yields for the first cumulant measured at a certain concentration that

$$\Gamma_1 / q^2 = D_c(q)$$

where $D_c(q)$ is an apparent, angular-dependent diffusion coefficient at the concentration c.

The slope of the apparent translational diffusion coefficient versus particle concentration gives k_d, the diffusional virial coefficient from the following relationship neglecting higher terms:

$$D(q) = D_0(1 + k_d C + ...)$$

where *C* is concentration

k_d is the diffusional virial coefficient

k_d is defined as
$$k_d = 2A_2 M_w - k_f - 2v_2$$

where A_2 is the second virial coefficient

M_w is the molecular weight

k_f is concentration dependence of the friction factor

And v_2 is the particle specific volume

10

All surfactant solutions were filtered through 0.2 µm Nalgene™ pore size filter (Nalge Nunc International Co.) using B-D syringe to remove dust. The first 5 ml filtered solution was discarded to avoid dilution of the filtrate due to the adsorption of surfactant on the filter membrane.

Dynamic light scatttering experiments were performed using the Brookhaven research grade system with a BI-9000 AT correlator and BI-200 SM geniometer with a detection angle of 90 degree. The water-cooled argon laser light source from Lexel Laser Inc. was used at a wavelength of 488 nm. The measurements were carried out at 25 ± 1^0C. The correlation function was measured and then analyzed using a cumulant analysis.
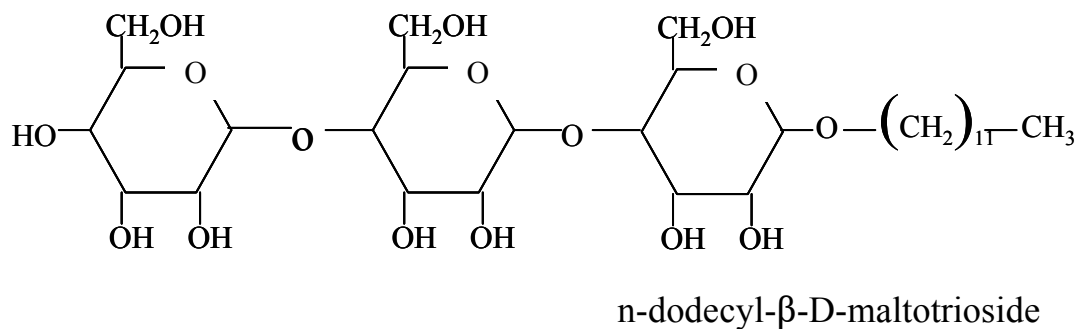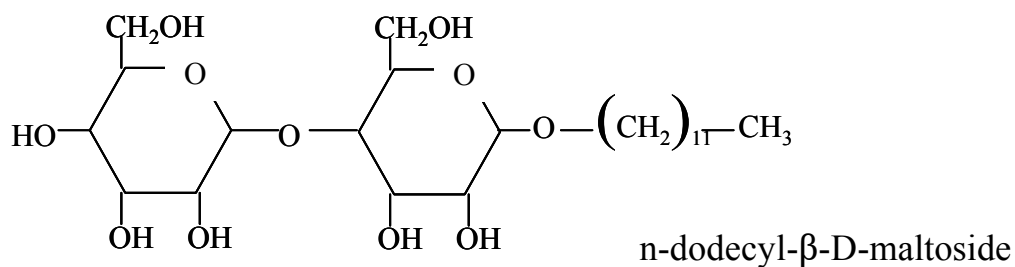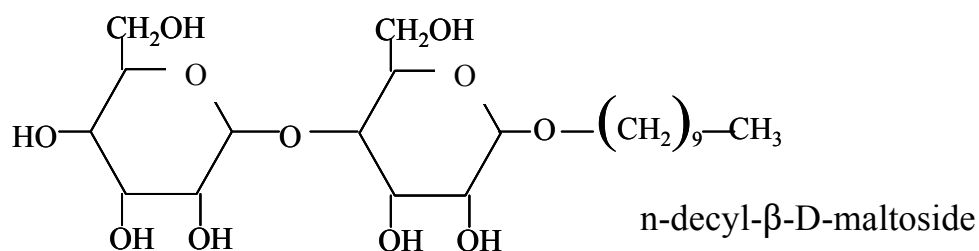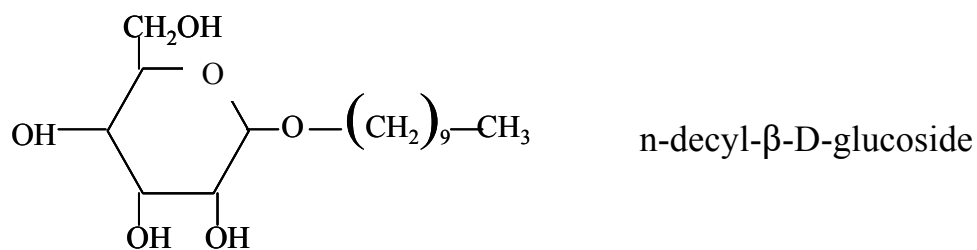
RESULTS AND DISCUSSION

1. Molar specific volume of several sugar-based surfactants

Information on partial specific volume of surfactants and their mixtures is required for treating analytical ultracentrifuge data. Previous results showed that the partial specific volume of n-dodecyl-β-D-maltoside determined by density gradient had a relatively large deviation (3%) from theoretical calculations based on Helmut Durchschlag's approach. To explore the reason for the discrepancy, the partial specific volumes of n-decyl-β-D-glucoside (C10G), n-decyl-β-D-maltoside(C10M) and n-dodecyl-β-D-maltotrioside (C12TM) were determined to correlate with that for n-dodecyl-β-D-maltoside(C12M). N-dodecyl-β-D-glucoside was not chosen due to its low solubility in water.

The above four surfactants are different in molecular structures with N-decyl-β-D-glucoside with only one glucose group as hydrophilic part and ten-carbon chain as hydrophobic part while N-dodecyl-β-D-maltoside has two glucose groups and n-dodecyl-β-D-maltotrioside three glucose groups, respectively. Both n-dodecyl-β-D-maltoside and n-dodecyl-β-D-maltotrioside contain twelve carbon in the hydrophobic parts. The molecular weights of n-decyl-β-D-glucoside, n-decyl-β-D-maltoside, n-dodecyl-β-D-maltoside and n-dodecyl-β-D-maltotrioside are 276.4, 482.6, 510.6 and 672.6, respectively.

The densities of the surfactant solutions are plotted as a function of concentration in figure 3. The density of n-decyl-β-D-glucoside is composed of two parts represented by the solid and dashed lines. Phase transition occurred at concentration over 0.015 g/cm^3. Hence the densities of turbid solutions were represented by dashed line.

n-decyl-β-D-glucoside

n-decyl-β-D-maltoside

n-dodecyl-β-D-maltoside

n-dodecyl-β-D-maltotrioside

Figure 2. Schematic display of structure of n-decyl-β-D-glucoside,

n-dodecyl-β-D-maltoside and n-dodecyl-β-D-maltotrioside.

Figure 3. Plot of density vs. concentration for n-decyl-β-D-glucoside, n-decyl-β-D-maltoside, n-dodecyl-β-D-maltoside, and dodecyl-β-D-maltotrioside at pH 6 and at 25˚C.

The slopes were used to calculate partial specific volumes:

$$\overline{v} = \frac{1}{\rho_0}\left(1 - \frac{d\rho}{dC}\right)$$

where C is surfactant volumeric concentration in g/ml, ρ and ρ_0 are the densities of the solution and the solvent, respectively and the results obtained are 0.809 cm³/g for n-decyl-β-D-glucoside, 0.820 cm³/g for n-dodecyl-β-D-maltoside, 0.775 cm³/g for n-decyl-β-D-maltoside and 0.892 for n-decyl-β-D-glucoside, respectively. It should be noted that only densities of clear solutions were used to obtain partial specific volume for n-decyl-β-D-glucoside.

The experimental result was compared with the theoretical data. Theoretical computation was based on the partial molar volume. Since the partial specific volume is obtained from:

$$\overline{v} = \overline{V}_C / M$$

The partial molar volume can be obtained by multiplying the partial specific volume with molecular weights.

14

On the other hand, the partial molar volumes of surfactants at 25°C can be calculated using the equation:

$$\overline{V_c} = \sum V_i + V_{CV} + \sum V_{RF} - \sum V_{ES}$$

where, V_i is the volume increment for any atom or atomic group, V_{CV} is the correction for the covolume, and V_{RF} and V_{ES} take into account the decrease in volume caused by ring formation and ionization (electrostriction), respectively.

The calculated and empirical results are compared in Table 1.

Table 1. Theoretical and experimental results of partial molar volumes and related parameters for n-decyl-β-D-glucoside, n-decyl-β-D-maltoside, n-dodecyl-β-D-maltoside and n-dodecyl-β-D-maltotrioside at pH 6 at 25°C.

	C	H	O1	O2	O3	CV	RF	$\overline{V}_C$(Theory)	$\overline{V}_C$(Exp.)	Difference	V per ring
C10G	16	32	2	1	3	12.4	1	276.4	285.8	9.4	9.4
C10M	22	42	4	2	5	12.4	2	372.8	390.3	17.5	8.7
C12M	24	46	4	2	5	12.4	2	405	418.7	13.7	6.8
C12TM	30	57	6	3	7	12.4	3	504.5	521.3	16.8	5.6

In this table, C, H, O1, O2, O3 are the number of carbon, hydrogen, oxygen atoms in the ether and in the ring, first OH for carbon, tertiary OH for carbon, respectively. CV was covolume. RF is for the ring formation. The next column was partial molar volume by theory. $\overline{V}_C$(Exp.) is the partial molar volume from experiments. The discrepancy between $\overline{V}$(theory) and $\overline{V}$(exp.) Is shown in "difference", which is divided by number of sugar groups and the results are noted as in "V per ring".
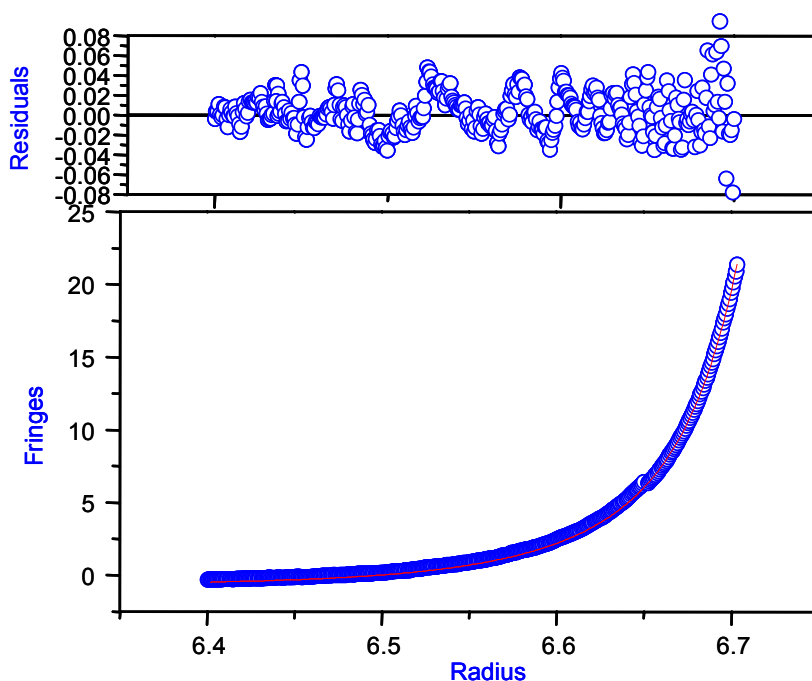
It is very interesting that V per ring followed the order: C10G>C10M>C12M>C12TM. The angle between two sugar groups with β-conformation was found to change from theoretical prediction. Both C10G and C10M have the same hydrocarbon chain with the difference resulting

only from the glucose group. It is clear that the glucoside can be rotated more easily than maltoside with two glucose groups and maltoside is prone to bend over than maltotrioside with three glucose groups. In the case of C10M and C12M, while the glucose groups are the same, the hydrocarbon chain length varies. The larger difference in partial molar volumes for C10M than that for C12M is possibly due to the fact that short hydrocarbon chain gives glucose groups more free space to turn. In other words, the glucose groups with short hydrocarbon chain is less restrained. Since a 1% deviation in partial specific volume will result in a 4% difference in molecular weight and the analytical ultracentrifugation data itself has around 10% error, the experimental method is considered reliable for systems containing sugar-based surfactants. The large deviation in partial molar volumes of sugar-based surfactants determined empirically from those obtained by theoretical calculation indirectly supports the bending conformation of glucose groups in aqueous solutions.

2. Analytical ultracentrifugation study of nonionic surfactant mixtures

A typical analytical diagram of sedimentation equilibrium experiment is exhibited in figure 4. The graph is made up of four parts: subject (name of the material and rotor speed), residual vs. radius plot, sedimentation equilibrium results together with the fitted curve, analytical results and experimental conditions.

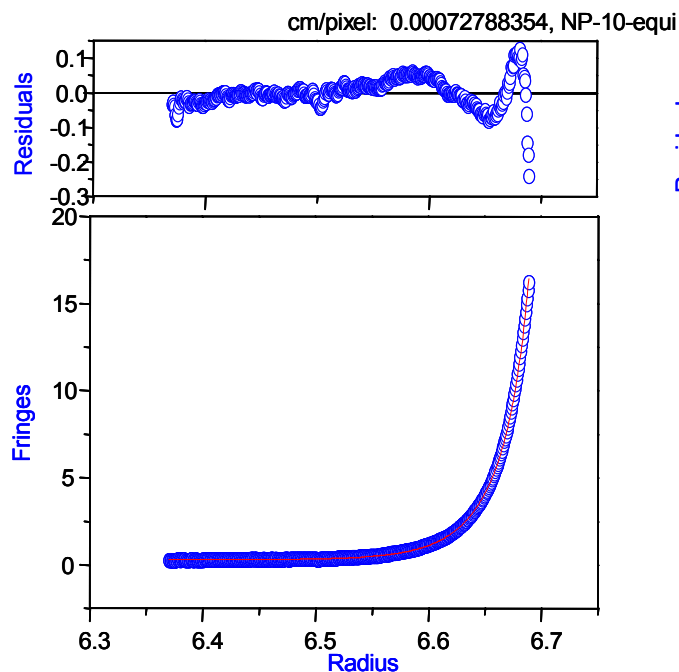DOF = 410   Variance = 4.06347E-4   Speed = 24000
Fitted Parameters: Time   = 332943
Co   Offset   Temp = 25
0.167   -0.455   V-bar = 0.877
M = 67058   B = 0   Rho   = 0.99727
N2 = 2.75   Ka2 = 0.013
N3 = 3.00   Ka3 = 1E-20
N4 = 4.00   Ka4 = 1E-20

Figure 4. Data for 0.03 M mixed surfactant solution of n-dodecyl-β-D-maltoside and nonyl phenol ethoxylated decyl ether of 1:1 molar ratio at rotor speed of 24k and temperature of 25°C.

DOF is the degree of freedom and the small variance suggests a successful fit. Among the

fitted parameters, Co is the fitted concentration of micelle. The aggregation number is obtained by

dividing micellar mass, M, by molecular weight of this surfactant. B is the second virial coefficient,

N_2 the stoichiometry of species 2 and K_2 the association constant for transition from species 1 to

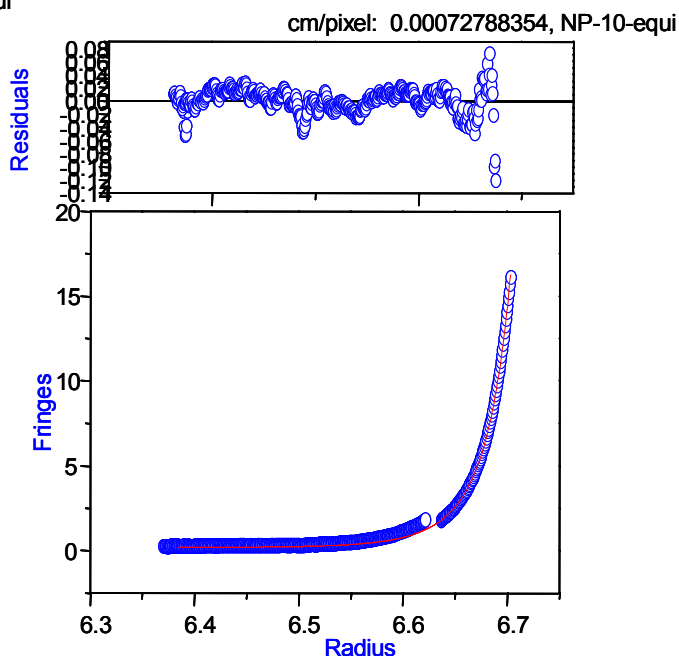species 2. N_3 and K_3 are similar to N and K for species 3.

In real cases, both nonideality and association are possible. They could be distinguished by checking the residuals and variance. As mentioned in experimental section, the second virial coefficient is an indication of the nonideality and could be determined from the variation of apparent micellar mass with concentration. Here is an example.

Model : Self Association
Data Set: equil/np-10/40K-B2

cm/pixel: 0.00072788354, NP-10-equi

DOF = 435	Variance = 0.0015	Speed = 40000
Fitted Parameters:		Time = 583627
Co Offset		Temp = 25
1E-3 0.282		V-bar = 0.92
M = 76472	B = -3.08E-7	Rho = 0.99723
N2 = 2.00	Ka2 = 1E-20	
N3 = 3.00	Ka3 = 1E-20	
N4 = 4.00	Ka4 = 1E-20	

Model : Self Association
Data Set: equil/np-10/40K-B2

cm/pixel: 0.00072788354, NP-10-equi

DOF = 433	Variance = 3.42271E-4	Speed = 40000
Fitted Parameters:		Time = 583627
Co Offset		Temp = 25
0.003 0.253		V-bar = 0.92
M = 62345	B = 0	Rho = 0.99723
N2 = 2.23	Ka2 = 0.125	
N3 = 3.00	Ka3 = 1E-20	
N4 = 4.00	Ka4 = 1E-20	

Figure 5. Data for the analysis of sedimentation equilibrium of nonyl phenol ethoxylated decyl ether at a concentration of 0.003M, rotor speed of 40k , at pH 6 and temperature of 25°C. The left one fitted micellar mass and second virial coefficient and the right one used micellar mass and association.

Two different protocols are used for the analysis of nonyl phenol ethoxylated decyl ether at a concentration of 0.03M, rotor speed of 40k and temperature of 25°C. Micellar mass and second virial coefficient are selected for the analysis shown on the left hand side, micellar mass and

association for the same data shown on the right side. Evidently, the residual plot on the left shows less variation than the right one. In addition, the variance of the fit on the left larger than that for the right. The nonideality was usually due to large excluded volume and charge of particles. Since nonyl phenol ethoxylated decyl ether has no charge, the second virial coefficient of its micelles is quite small, $-3*10^{-7}$. This value is lower than the minimum requirement for nonideality. Both residual plot and variance support the presence of multi-species in nonyl phenol ethoxylated decyl ether aqueous solution at this concentration.

All sedimentation equilibrium analytical results are illustrated in Table 2. Different rotor speeds were tried for each surfactant concentration at several rotor speeds. The aggregation number of micelles are given next to the rotor speed. It should be noted that n-dodecyl-β-D-maltoside exihibits only one type of micelle. Two types of micelles were found for nonyl phenol ethoxylated decyl ether and for the 1:1 molar ratio mixture. Range of aggregation number for each species are specified on the table.

Table 2. Sedimentation equilibrium analytical results for n-dodecyl-β-D-maltoside, nonyl phenol ethoxylated decyl ether and their 1:1 mixture at different concentrations and rotor speeds.

DM	Rotor speed	C=0.024M Aggregation number	C=0.012M Aggregation number	C=0.004M Aggregation number
	16k	157	151	152
	32k	148	148	163
	40k	147	140	132

NP	Rotor speed	C=0.006M Aggregation number		C=0.003M Aggregation number		C=0.001M Aggregation number	
		I	II	I	II	I	II
	16k	118	406	121	356	78	N/A
	32k	106	312	101	246	98	N/A
	40k	91	264	94	210	95	N/A

1:1 Mixture	Rotor speed	C=0.006M Aggregation number		C=0.003M Aggregation number		C=0.001M Aggregation number	
		I	II	I	II	I	II
	16k	52	384	45	321	72	352
	24k	119	345	114	315	89	216
	32k	111	293	95	221	112	311
	40k	109	298	62	158	117	454

The average aggregation number of DM micelle is 148±9. The value reported from small angle neutron scattering studies for n-dodecyl-β-D-maltoside is 113-129 [9]. The effect of rotor speed on aggregation number of n-dodecyl-β-D-maltoside can be seen in Figure 6 to be small. Nonyl phenol ethoxylated decyl ether has the average aggregation number of 100±13 for species 1 and 299±73 for species 2. There are two different values in the literature for the aggregation number of nonyl phenol ethoxylated decyl ether. One was 100[10] and the other 276 [11]. Although both values were obtained using light scattering technique, only one value was reported in each paper. Our data yields both of these two. Aggregation number of their 1:1 mixtures had relative large deviations, i.e., 92±27 for species 1 and 306±79 for species 2.
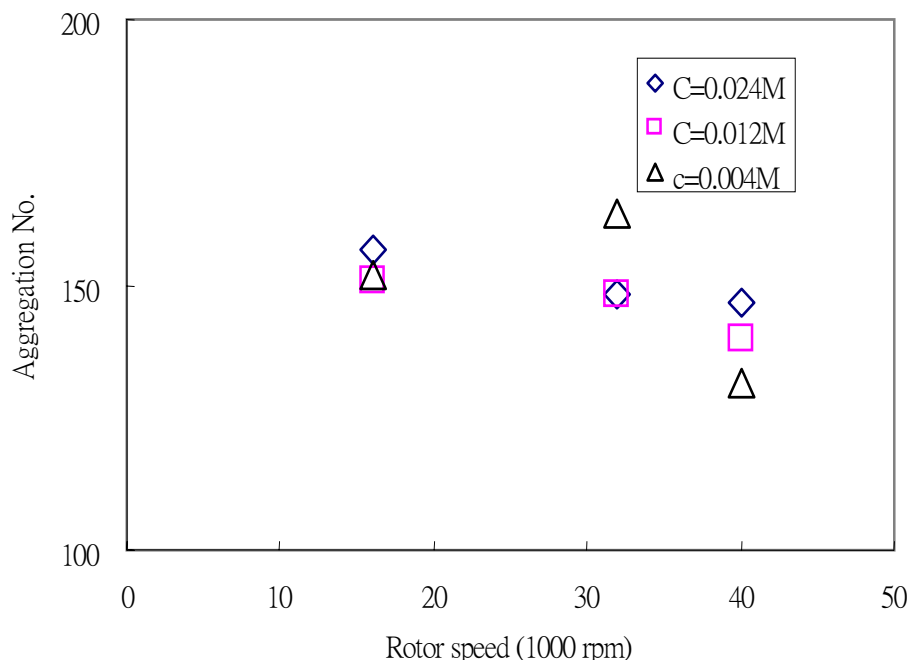

Figure 6. Aggregation number of n-dodecyl-β-D-maltoside at different rotor speeds at 25°C.

The coexistence of two micellar species in the case of nonyl phenol ethoxylated decyl ether is possibly related to its structure. A recent study has shown that polyethylene surfactant can form network structures in L_1 region [12]. Thus, the behavior of polyethylene surfactant is similar to that of the polymer in certain concentration range. The long flexible polyethylene chain is responsible for the network formation and the polymer like behavior. Thermodynamical consideration suggests only one type of micelles to exist [13]. However, our study reveals, for the first time, the small micelles to coexist with the big micelles at high concentrations. The large size of the mixed micelles provides more space inside the micelles to trap crude oil. If the behavior of surfactant mixtures is similar to that of the polymer-like nonyl phenol ethoxylated decyl ether, the dosage of polymer for EOR may be reduced since the mixed surfactant itself can be adjusted for viscosity. In general, both the large micellar size and resulting polymer-like behavior could potentially benefit enhanced oil recovery process.

3. Study of nonionic surfactants and their mixtures using dynamic light scattering

The apparent diffusion coefficients of DM, NP-10 and their 1:1 mixture were determined to change with concentration as shown in Figure 7 using the dynamic light scattering technique.
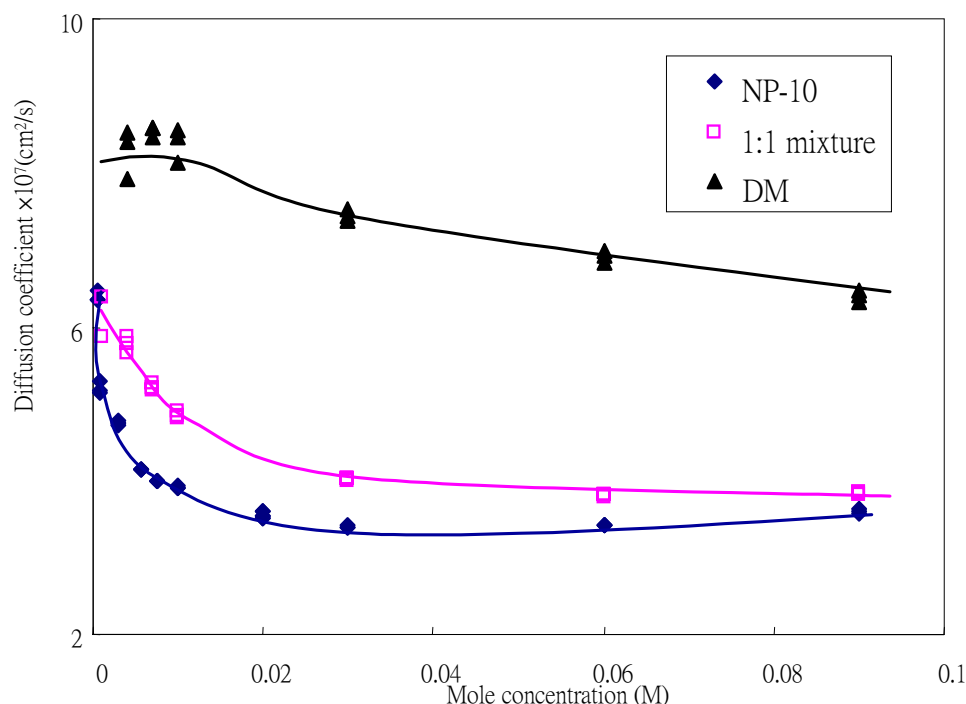
Figure 7. Diffusion coefficients of nonyl phenol ethoxylated decyl ether, n-dodecyl-β-D-maltoside and their 1:1 mixtures as a function of mole concentration at 25°C

Movement of n-dodecyl-β-D-maltoside micelles are faster than those of nonyl phenol ethoxylated decyl ether and their mixtures. Initially, apparent diffusion coefficient of n-dodecyl-β-D-maltoside micelles remained constant followed by a decrease at higher concentrations. Nonyl phenol ethoxylated decyl ether and their mixture exhibited a different behavior, the apparent diffusion coefficient decreased sharply at low concentrations itself. A negative slope of the D vs. C curve usually suggests formation of bigger aggregates. At high concentrations, the intermicellar interaction affects the micellar mobility. Such solutions should be treated as semi-dilute instead of dilute.

SUMMARY AND CONCLUSIONS

It is the aim of this project to develop a knowledge of structure -- performance relationships. During this period, partial specific volume of four sugar-based surfactants were determined Analytical ultracentrifuge equilibrium experiment was done for the investigation of the nature and distribution of surfactant micelles. Dynamic light scattering was also employed for the determination of apparent diffusion coefficients. The results obtained are summarized below:

1.   Partial Specific volume V per sugar ring of n-decyl-β-D-glucoside, n-decyl-β-D-maltoside, n-dodecyl-β-D-maltoside and n-dodecyl-β-D-maltotrioside followed the order: C10G>C10M>C12M>C12TM. The variation could be accounted for by considering the flexibility of β-conformation sugar group in the solution. The easier the sugar-group can turn over, the larger the error. Experimental method is suggested to minimize the deviation in systems containing sugar-based-surfactants.

2.   From sedimentation equilibrium experiments, both nonyl phenol ethoxylated decyl ether and its mixtures with n-dodecyl-β-D-maltoside were found to have two types of micelles. The average aggregation number of n-dodecyl-β-D-maltoside, nonyl phenol ethoxylated decyl ether and their mixtures are 148±9, 100±13 (species 1) and 299±73 (species 2) and 92±27 (species 1) and 306±79 (species 2), respectively. Two different aggregation number of 100 and 276 are reported in literatures for nonyl phenol ethoxylated decyl ether. Our study revealed, for the first time, that small micelles can coexist with larger micelles at high concentrations due to the unique structure of the surfactant. The implication of this finding lies in the fact that efficiency of oil recovery can be improved due to the large micellar size and its polymer-like viscosity and oil solubilization.

23

3.　　Analysis of the apparent diffusion coefficients of n-dodecyl-β-D-maltoside, nonyl phenol ethoxylated decyl ether and their 1:1 mixtures obtained using the dynamic light scattering technique indicates aggregate formation in solutions, supporting the sedimentation equilibrium results

FUTURE PLANS

For task 2:

*　　To validate the viscoelastic property of surfactant mixture, the viscosity of the surfactant mixture will be examined and compared with that of the polymer.

*　　Conduct dynamic light scattering experiment to determine active energy for diffusion and develop the relationship of diffusion coefficient to the volumetric fraction.

*　　Our previous result showed the nonideality of surfactant mixture using ultra-filtration technique, the mixing ratio of each surfactant component over the other one in mixed micelles will be measured to explore the nonideality for n-dodecyl-β-D-maltoside, nonyl phenol ethoxylated decyl ether and their 1:1 mixtures

For task 3:

*　　Since coexistence of multi-species can also be detected using sedimentation velocity technique, it is planed to run sedimentation velocity experiment for n-dodecyl-β-D-maltoside, nonyl phenol ethoxylated decyl ether and their 1:1 mixtures .

Reference

1. Lei Huang and P. Somasundaran, Langmuir 1996, 12, 5790-5795

2. Helmut Durchschlag and Peter Zipper, "calculation of the partial volumes of organic compounds and polymers", Progress in Colloid & Polymer Science, 94 (1994), 20-39

3. Helmut Durchschlag and Peter Zipper, "Calculation of partial specific volumes of detergents and lipids", Jorn. Com. Esp. Deterg., 26 (1995), 275-292

4. Allen Furst, Beckman Coutler's website, "Overview of sedimentation velocity for the Optima^{TM} XL-A analytical ultracentrifuge"

5. Allen T. Ansevin, Dennis E. Roark and David A. Yphantis, "Improved ultracentrifuge cells for high-speed sedimentation equilibrium studies with interference optics", Analytical biochemistry 34, 237-261, (1970)

6. http://www.sciences.salford.ac.uk/chemist/LecNotes/Bloor%20DM/Colloids/Lect2.pdf

7. Tom Wines, PhD thesis, Columbia University, 2002

8. D. K. McRorie, and P. J. VoelkerAnalytical ultracentrifugation, Vol. 2: Self-associating systems in the analytical ultracentrifuge,1993

9. S. Bucci, C. Fagotti, V. Degiorgio, and R. Pianza, Langmuir 7: 824 (1991)

10. J. Schick, J. Phys. Chem. 66, 1326, 1962

11. C. W. Dwiggins, J. Phys. Chem. 64, 1175 (1960)

12.Bernheim-Groswasser, A.; Wachtel, E.; Talmon, Y.; Langmuir; 2000; 16(9); 4131-4140

13. W. E. McMullen, W. M. Gelbert and A.Ben-Shaul in Micelles, membranes, microemulsions, and monolayer, (W. M Gelbart, A. Ben-Shaul, D. Roux Ed.), Springer-Verlag, 1994

14. Martin Pisárčik, Ferdinand Devínsky, Emil Švajdlenka, Colloids and surfaces, A, 119, 1996, 115-122

Publications and presentations

1. R. Zhang, L. Zhang and P. Somasundaran. "Surface tension and fluorescence study of n-dodecyl-β-D-maltoside with anion, cationic and nonionic surfactant mixtures in aqueous solution", submitted)

2. L. Zhang, P. Somasundaran, J. Mielczarski, and E. Mielczarski, "Adsorption mechanism of n-dodecyl-β-D-maltoside on alumina", Journal of Colloid and interface science 256, 16-22, (2002)